

Supporting Information

Cargo Release from Non-Enveloped Viruses and Virus-Like Nanoparticles: Capsid Rupture or Pore Formation

Lukáš Sukeník,^{†,‡} Liya Mukhamedova,[†] Michaela Procházková,[†] Karel Škubník,[†]
Pavel Plevka,[†] and Robert Vácha*,^{†,‡,¶}

[†] CEITEC – Central European Institute of Technology, Masaryk University,
Kamenice 753/5, 625 00 Brno, Czech Republic

[‡] National Centre for Biomolecular Research, Faculty of Science, Masaryk University,
Kamenice 5, 625 00 Brno, Czech Republic

[¶] Department of Condensed Matter Physics, Faculty of Science, Masaryk University,
Kotlářská 267/2, 611 37 Brno, Czech Republic

E-mail: robert.vacha@mail.muni.cz

```
import os

for e, entry in enumerate(sorted(os.listdir('./'))):
    if entry[-3:] != 'png':
        continue
    pdb.file_png_load(entry, entry)
    image = gimp.image_list()[0]

    image.add_layer(image.layers[0].copy(True), -1)
    image.add_layer(image.layers[1].copy(True), -1)

    pdb.gimp_layer_set_mode(image.layers[0], 23) # 23 = overlay
    pdb.gimp_layer_set_opacity(image.layers[0], 100) # 100%

    pdb.plugin_sel_gauss(image, image.layers[0], 25, 255)
    pdb.gimp_drawable_levels_stretch(image.layers[0])

    pdb.gimp_edit_copy_visible(image)
    image = pdb.gimp_edit_paste_as_new()

    output = 'proc_'+entry

    pdb.file_png_save(image, image.layers[0], output, output, 0, 9, 0, 0, 0, 0, 0)
    [gimp.pdb.gimp_image_delete(image) for image in gimp.image_list()]

pdb.gimp_quit(0)
```

Listing 1: Gimp script to enhance cryo-EM micrographs.

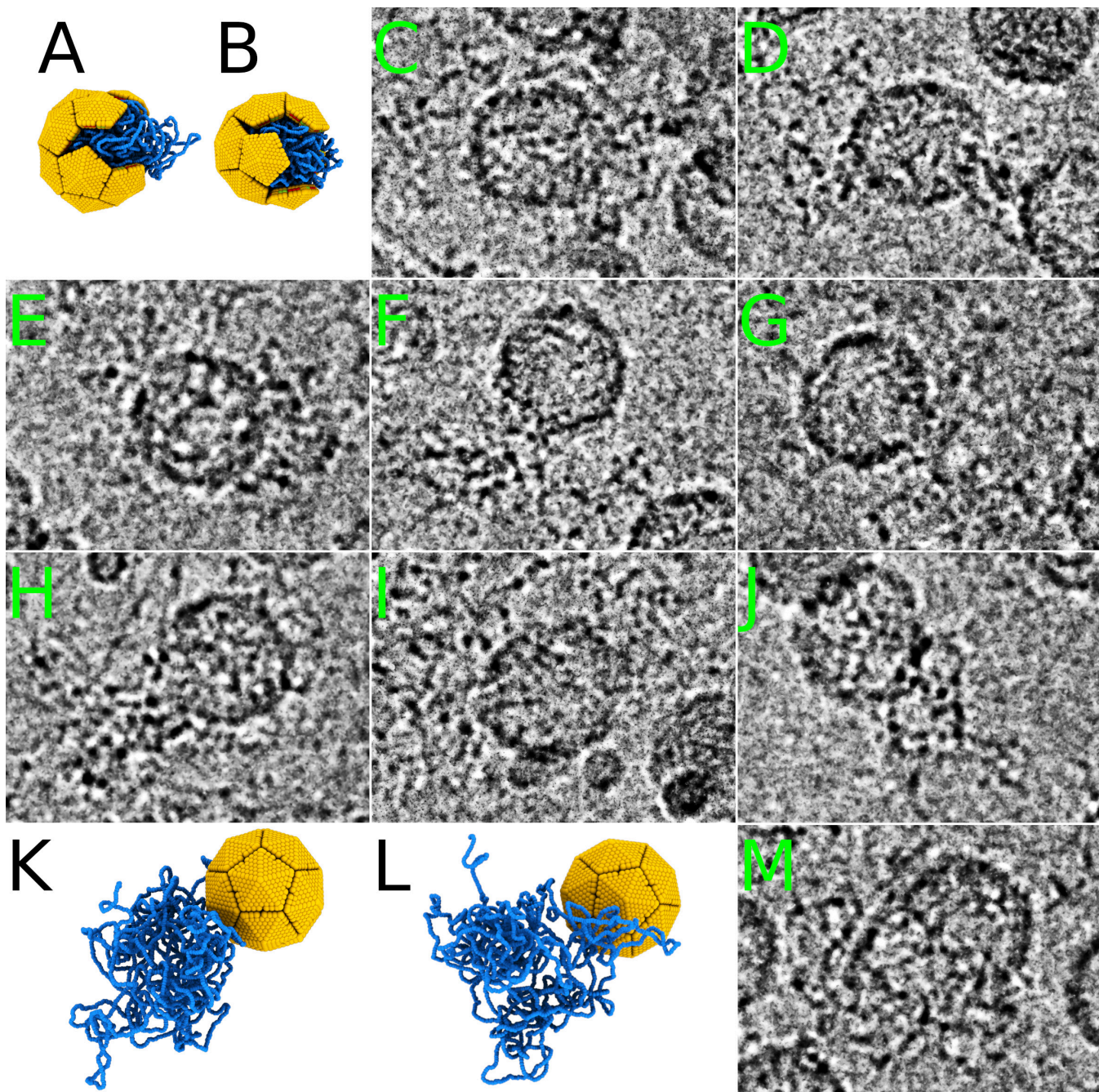


Figure S1: Comparison of simulated structures and selected viral capsids from cryo-EM micrographs. The cryo-Em data of virus SBV suggested similar structures as in the rupture and bloom pathways. (A) was a representative structure of the rupture release pathway at 3 ns after opening. (B) was a representative structure of the bloom release pathway at 2 ns after opening. (C-J) were structures of SBV virus from cryo-EM micrographs. (K) was rupture release at 100 ns. (L) was bloom release at 100 ns. (M) showed a non-compact genome close to an empty SBV capsid. Unfortunately, due to the nature of the cryo-EM method, transient intermediates are characterized with low resolution. Additionally, the causal link of the genome being near a capsid, as in (M), can only be speculated upon.

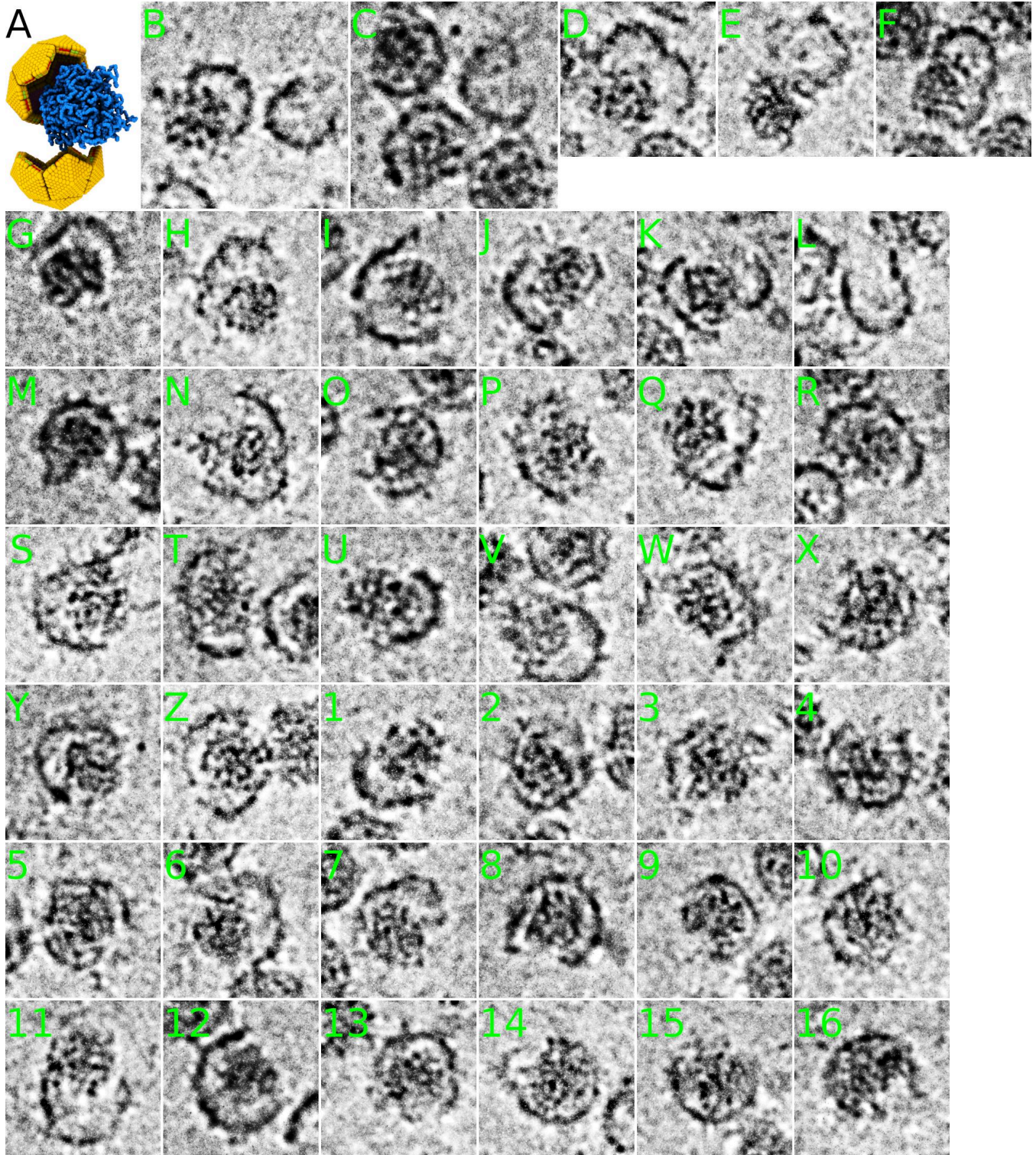


Figure S2: Comparison of simulated structure and selected viral capsids from cryo-EM micrographs. The cryo-Em data of virus DWV suggested similar structures as in the burst release with a compact genome. (A) was a representative structure of the burst release pathway at 100 ns after breaking apart. (B-16) were structures of DWV virus from cryo-EM micrographs.

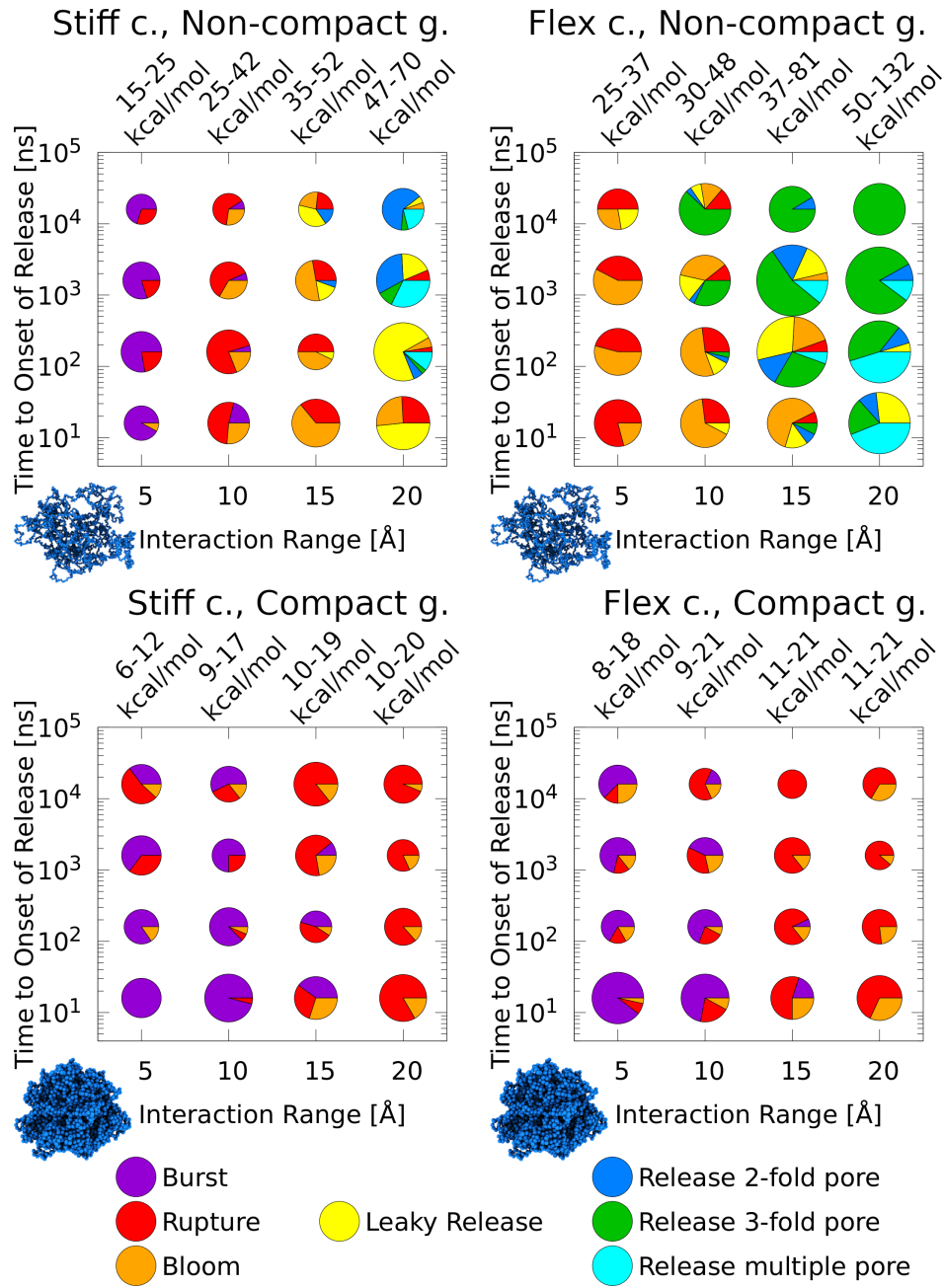


Figure S3: Diagram of release pathway incidence as a function of interaction range and sorted according to time necessary for release onset. There were 7 different release pathways – denoted with different colors in the legend. We varied 4 different virus-like nanoparticle/virus properties: (A) stiff capsid with non-compact genome, (B) flexible capsid with non-compact genome, (C) stiff capsid with compact genome, (D) flexible capsid with a compact genome. Pentamer interaction strength increased proportionally with the increase in interaction range to keep the capsid stability roughly equal for all studied models, *i.e.* a similar time to the onset of release. The investigated interaction strengths for a given interaction range are displayed above each plot. The increased pentamer interaction strength increased capsid stability, but only slightly changed the release pathway. The number of simulations per pie chart was 9–55. The time boundaries the pie charts represents are 5–50, 50–500, 500–5000, and 5000–100 000 ns. The area of the pie charts scale with the number of simulations they represent.

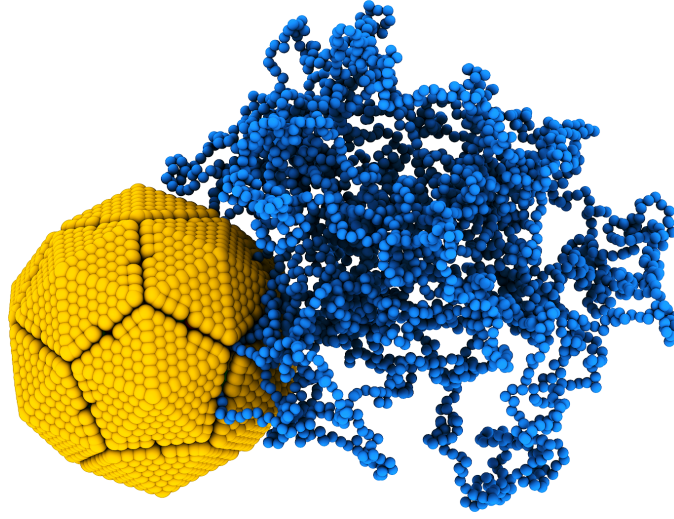


Figure S4: Example of arrested release, where the genome was clamped by the capsid, preventing further release. About 15 % of the genome remained inside the capsid.

Table S1: Table of fit values for supplementary Figure S6. The simulation results were fitted to the Arrhenius equation $k = A \cdot \exp(\frac{E_A \cdot x}{R \cdot T})$, where A is the frequency factor, E_A a scaling factor of activation energy (interaction strength in our case), R is the gas constant and T is the temperature. First, 9 simulations of genome release were performed for each value of activation energy $E_A \cdot x$. The rate constant, k , was calculated from the half-life using the equation $k = \frac{\ln 2}{\tau_{1/2}}$ for each activation energy $E_A \cdot x$. Then, the fit to the Arrhenius equation was performed using the calculated rate constant, taking into consideration both the error of the rate constant and the thermal fluctuations of activation energy $E_A \cdot x$.

Release type	Genome type	Capsid stiffness	Interaction range [Å]	E_A	E_A error	Relative error E_A [%]	A [ns ⁻¹]	A error [ns ⁻¹]	Relative error A [%]
Rapid	Non-compact	Rigid	5	0.65	0.08	12.2	$1 \cdot 10^{-8}$	$4 \cdot 10^{-8}$	295
Rapid	Non-compact	Rigid	10	0.47	0.05	10.4	$1 \cdot 10^{-10}$	$4 \cdot 10^{-10}$	289
Rapid	Non-compact	Rigid	15	0.44	0.04	9.6	$1 \cdot 10^{-12}$	$5 \cdot 10^{-12}$	314
Rapid	Non-compact	Rigid	20	0.244	0.007	3.1	$13 \cdot 10^{-9}$	$9 \cdot 10^{-9}$	68
Rapid	Non-compact	Flexible	5	0.42	0.02	3.7	$6 \cdot 10^{-8}$	$5 \cdot 10^{-8}$	83
Rapid	Non-compact	Flexible	10	0.33	0.05	14.6	$1 \cdot 10^{-7}$	$2 \cdot 10^{-7}$	295
Rapid	Non-compact	Flexible	15	0.3	0.02	6.7	$2 \cdot 10^{-8}$	$3 \cdot 10^{-8}$	142
Rapid	Non-compact	Flexible	20	-	-	-	-	-	-
Rapid	Compact	Rigid	5	0.98	0.06	6.5	$1 \cdot 10^{-5}$	$1 \cdot 10^{-5}$	108
Rapid	Compact	Rigid	10	0.7	0.1	13.9	$1 \cdot 10^{-5}$	$2 \cdot 10^{-5}$	224
Rapid	Compact	Rigid	15	0.66	0.06	9.6	$6 \cdot 10^{-6}$	$9 \cdot 10^{-6}$	162
Rapid	Compact	Rigid	20	0.61	0.06	9.7	$2 \cdot 10^{-5}$	$3 \cdot 10^{-5}$	142
Rapid	Compact	Flexible	5	0.84	0.07	8.2	$1 \cdot 10^{-6}$	$1 \cdot 10^{-6}$	159
Rapid	Compact	Flexible	10	0.7	0.07	9.9	$3 \cdot 10^{-6}$	$5 \cdot 10^{-6}$	173
Rapid	Compact	Flexible	15	0.69	0.05	7.0	$2 \cdot 10^{-6}$	$3 \cdot 10^{-6}$	130
Rapid	Compact	Flexible	20	0.63	0.07	10.7	$1 \cdot 10^{-5}$	$1 \cdot 10^{-5}$	183
Slow	Non-compact	Rigid	5	-	-	-	-	-	-
Slow	Non-compact	Rigid	10	-	-	-	-	-	-
Slow	Non-compact	Rigid	15	-	-	-	-	-	-
Slow	Non-compact	Rigid	20	0.23	0.02	7.0	$4 \cdot 10^{-8}$	$7 \cdot 10^{-8}$	163
Slow	Non-compact	Flexible	5	-	-	-	-	-	-
Slow	Non-compact	Flexible	10	-	-	-	-	-	-
Slow	Non-compact	Flexible	15	0.07	0.01	18.4	1	1	122
Slow	Non-compact	Flexible	20	0.064	0.003	4.8	0.023	0.001	44
Slow	Compact	Rigid	5	-	-	-	-	-	-
Slow	Compact	Rigid	10	-	-	-	-	-	-
Slow	Compact	Rigid	15	-	-	-	-	-	-
Slow	Compact	Rigid	20	-	-	-	-	-	-
Slow	Compact	Flexible	5	-	-	-	-	-	-
Slow	Compact	Flexible	10	-	-	-	-	-	-
Slow	Compact	Flexible	15	-	-	-	-	-	-
Slow	Compact	Flexible	20	-	-	-	-	-	-

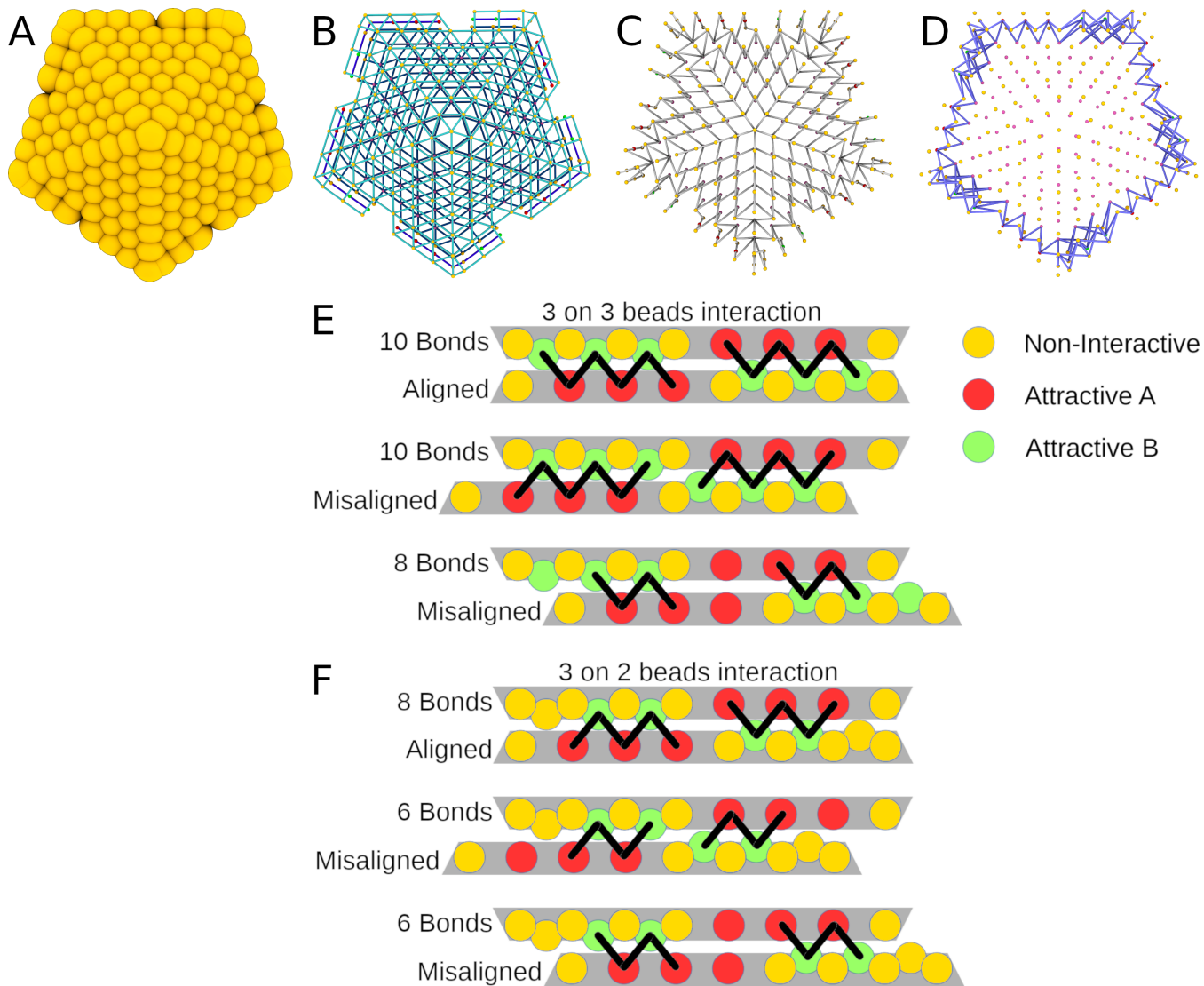


Figure S5: Illustration of pentamer pseudoatom layout and bond scaffolding. All beads are purely repulsive, with the exception of the red and green ones. (A) View from outside the capsid. (B) bonds holding a single layer together. (C) Cross-layer bonds. (D) Bonds preventing lateral movement of interface beads. The use of three A (red) and three B (green) attractive beads at the pentamer edge (E) leads to a degenerated state with the same energy, where the pentamers are misaligned/shifted. To prevent the misaligned states, we used three A and two B beads at the pentamer edge (F).

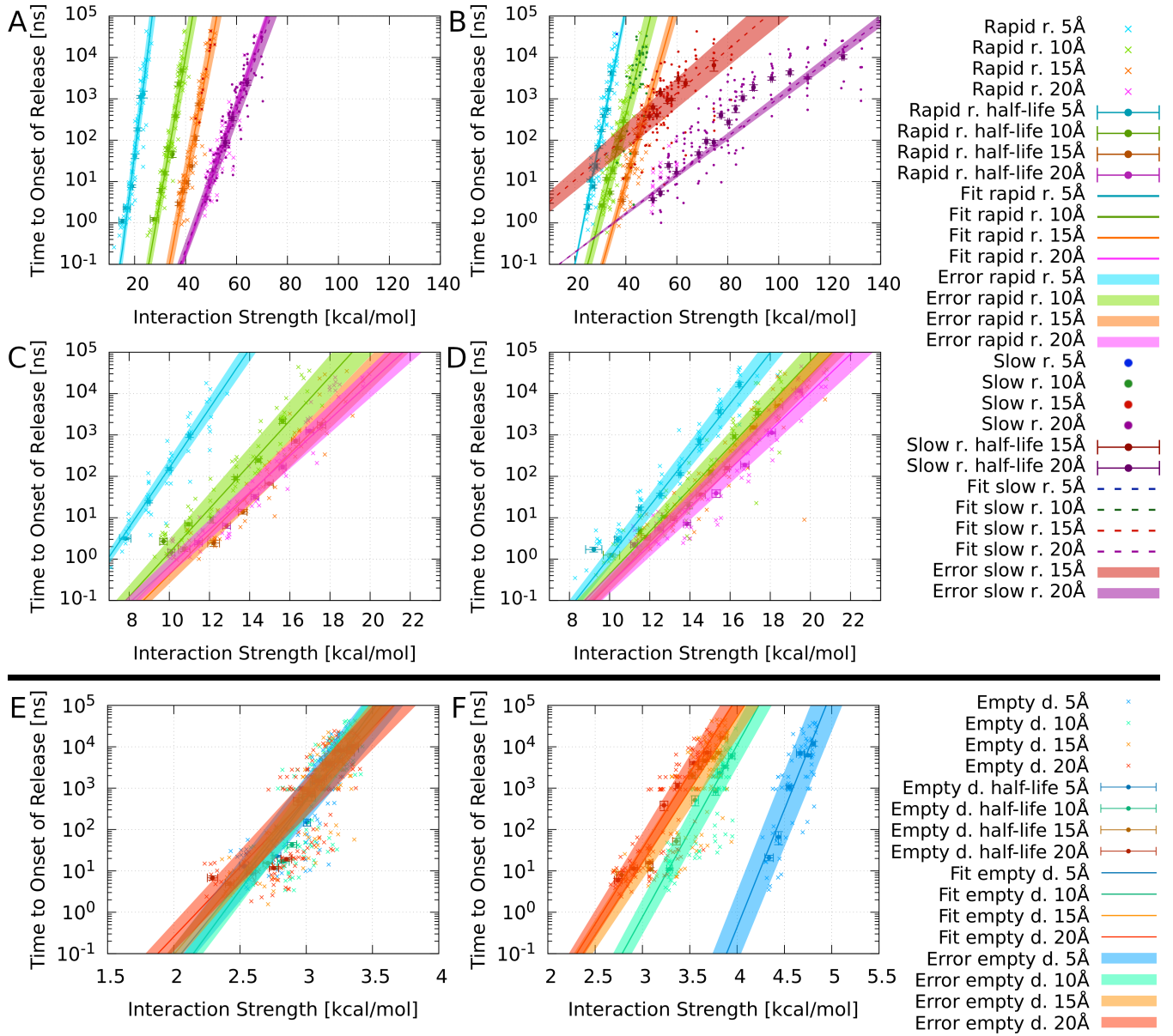


Figure S6: Graphs of time to genome release (or capsid dissociation) as a function of pentamer-pentamer interaction strength obtained from simulations and fitted to Arrhenius equation. **A** Rigid capsid with non-compact genome. **B** Flexible capsid with non-compact genome. **C** Rigid capsid with compact genome. **D** Flexible capsid with compact genome. **E** Dissociation of rigid capsid without a genome. **F** Dissociation flexible capsid without a genome.